

pubs.acs.org/JPCA Article

Laser Spectroscopy of Helium Solvated Clusters of Methanol and Methanol—Water in the Symmetric Methyl Stretching Band

Published as part of The Journal of Physical Chemistry virtual special issue "Early-Career and Emerging Researchers in Physical Chemistry Volume 2".

Maameyaa Asiamah and Paul L. Raston*



Cite This: J. Phys. Chem. A 2023, 127, 946-955



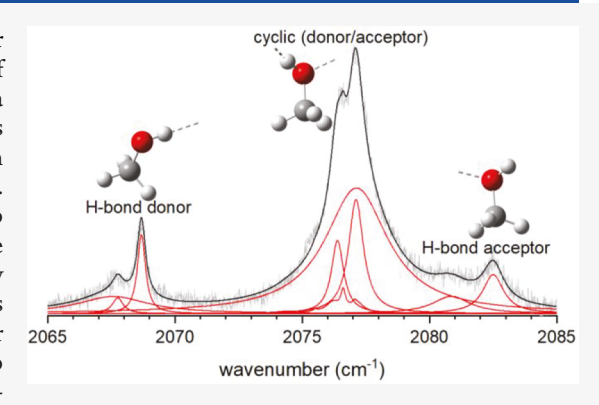
ACCESS

III Metrics & More

Article Recommendations

Supporting Information

ABSTRACT: Mid-infrared spectra of methanol and methanol—water clusters have been investigated in the symmetric CD₃ stretching band of CD₃OH and CD₃OD. We find that the position of this band provides a useful signature of the general type of hydrogen-bonded cluster it is associated with. Our results are consistent with those previously reported in the OH stretching region (Sulaiman, M. I.; Yang, S.; Ellis, A. M. J. Phys. Chem. A 2017, 121, 771–776) in that methanol clusters from the trimer to the pentamer are cyclic and that mixed clusters with one water molecule (and at least two methanol molecules) are also cyclic. We additionally provide evidence that the methanol trimer adopts a chair-like structure (as opposed to bowl-like), that mixed clusters with a larger number of water molecules are also cyclic, and that branched methanol clusters contribute to the depletion signal in larger methanol clusters. We performed double-hybrid DFT calculations which support these interpretations.



1. INTRODUCTION

The microscopic hydrogen-bonding (H-bonding) networks within liquid water and various alcohols have a relatively high degree of local orientational ordering, which plays an important role in determining their physicochemical properties.^{1,2} H-bonding motifs within these types of networks are typically described in terms of "linear" and branched chains³ and rings.4 There has been considerable debate as to the relative abundance of these types of motifs in both pure liquids and solution. For example, comparison of calculations with experimental data has led to the conclusion that liquid methanol predominantly consists of long winding chains, ring structures ("cyclic and/or lasso"), or a mixture of chains and rings (with six and/or eight molecules). More recently, a Raman spectroscopic study has provided information about the average cluster sizes in liquid methanol, with indications that the trimer, tetramer, and pentamer make up >50% of the total clusters.8 This broad distribution in H-bonded cluster sizes (and structures) makes gaining detailed experimental insight into the types of microscopic environments that exist in simple molecular liquids difficult (since measurements typically probe the ensemble average).

While the spectroscopic investigation of isolated clusters does not provide direct information regarding the relative abundance of the structural aggregates (motifs) in solution, it can provide valuable insight into their structures and, with supporting theory, the energy landscapes that interconnect them. Isolated methanol clusters are typically formed in supersonic jet expansions, and the resulting molecular beams can be probed by a number of techniques, including microwave spectroscopy, Fourier transform infrared spectroscopy, and broadly, laser spectroscopy. These investigations, in concert with theory, have allowed for determination of the structures of various isomers of different methanol cluster sizes. The accuracy to which the structure can be determined depends on a number of factors, and while it is the highest based on microwave spectroscopy, measurements beyond the dimer are problematic on account of the low dipole moments of many of the lowest energy structural isomers (that are often ring-like).

Techniques that involve infrared spectroscopy have been most commonly used to probe methanol clusters, which can provide the characteristic vibrational frequencies for each isomer in the molecular beam. The vibrational frequencies are particularly sensitive to the arrangement of the molecules in

Received: November 28, 2022 Revised: January 5, 2023 Published: January 20, 2023





each cluster, especially the ones whose frequencies sensitively depend on the cluster size and H-bonding arrangement. The most sensitive vibrational mode is the OH stretch since it is often directly involved in H-bonding and therefore experiences the greatest shifts upon complexation. 20,21 However, this was not the first mode investigated in pure methanol clusters by laser spectroscopy, since the high power optical parametric oscillator (OPO) systems that are typically used in the OH stretching region were not developed until after the high power CO2 lasers that are well suited for investigating the CO stretching region. Spectra in the CO stretching region showed a sensitive dependence of the average vibrational frequency on the cluster size up to about the pentamer, while the band profiles are characteristically different between cluster sizes, up to at least the octamer. ^{22–28} This is qualitatively similar to what was subsequently observed in the OH stretching region, although the direction of the vibrational shift is different and magnitude of the shift is much greater. ^{26,29,30} These laser spectroscopic investigations, in agreement with electric deflection studies,³¹ showed that clusters beyond the dimer are ring-like, having very small dipole moments. 16,17

Helium nanodroplets present a gently perturbing medium within which higher energy structural isomers can be formed. This is on account of their low temperature (0.37 K³²) and exceptionally large thermal conductivity, which results in monomer units being cooled to almost 0 K before associating with each other and oftentimes trapping them in a local minimum. Well-known examples include the helium nanodroplet isolation of linear chains of HCN molecules³³ and the formation of the cyclic water hexamer.³⁴ Helium solvated methanol clusters have previously been investigated in both the CO stretching³⁵ and OH stretching³⁶ regions. In the CO stretching region, evidence for the dimer and trimer adopting the same configuration as in the gas phase was found, while for the tetramer and pentamer, branched ring-like structures were inferred from the spectra. This is in contrast to what was uncovered in the higher-resolution spectra more recently reported in the OH stretching region, which only show evidence for ring-like structures from the trimer to the pentamer.

In this article, after briefly introducing the technique, we discuss the quantum cascade (qc) laser spectra of methanol clusters in the symmetric CD_3 stretching region, then the less complicated methanol—water cluster spectra (in the same region). This is followed by a comparison of our results with those previously published in helium nanodroplets in the OH stretching region and a comparison with double-hybrid density functional theory (DFT) calculations. Part of the motivation of the series of experiments discussed here was to see if the much less sensitive symmetric CD_3 stretching mode could be probed in order to determine the general structure of methanol complexes formed in cold helium nanodroplets.

2. EXPERIMENTAL SECTION

2.1. Helium Nanodroplet Isolation Spectroscopy. Previously, we have provided detailed explanations of the experimental apparatus, $^{37-40}$ and so here we only briefly mention relevant aspects of it. The apparatus consists of a source chamber where helium nanodroplets consisting of a few thousand helium atoms are produced, 41,42 a pickup chamber where they are doped, and a detection chamber where they are analyzed. The nozzle in the source chamber was cooled to \sim 20 K with a closed cycle helium cryostat and backed with 34.5 bar

of ultrapure carrier grade (99.9995%) helium. Methanol-d₄ (99.5%) was used as received from Cambridge Isotope Laboratories, and methanol-d₃ (CD₃OH) was produced by mixing ethylene glycol and methanol- d_4 in a ratio of \sim 3:1. We used ethylene glycol for H/D exchange because each molecule contains two OH groups and the (pure) substance has a very low vapor pressure (\sim 0.1 mbar at ambient temperature). The methanol isotopologue was flowed into the pickup chamber by means of a Swagelok metering valve (SS-SS4). For co-doping experiments, a separate valve (same type) was used to control the flow of water; this valve was heated to prevent condensation. The pressure of water or methanol in this chamber was adjusted to vary the average number of molecules that were picked up by the nanodroplets, which allowed for the production of clusters ranging in size from about one to six. The doped droplets were characterized by depletion spectroscopy, which relies on the evaporative loss of helium atoms following absorption of infrared radiation at around 4.8 µm. The infrared light source was a quantum cascade laser, and we detected the relative size of the droplets with a quadrupole mass spectrometer operated in RF-only mode (ions with masses greater than ~6 u were transmitted). There are a number of review articles that cover the infrared spectroscopy of molecules and clusters embedded in helium nanodroplets and that provide additional details of the technique. 43-5

2.2. DFT Calculations of Methanol Clusters. In the previous helium nanodroplet investigation of methanol clusters (in the OH stretching region), calculations were performed at the MP2/AVDZ level except when convergence to a stable structure was not obtained, in which case the B3LYP/AVDZ level of theory was used.³⁶ Here, we performed optimization and frequency calculations using Gaussian 0953 at the same level of theory (B2PLYP-D3) for each cluster size/structure. This was done to facilitate a meaningful comparison of the calculated and experimental vibrational frequencies, since the vibrational shifts between different cluster sizes/isomers are inherently small in the symmetric CD3 stretching band. We used the B2PLYP-D3 method on account of it being much less computationally expensive than MP2 (and so larger cluster calculations were feasible), and this comes at a relatively small cost in terms of accuracy. We used a double-hybrid functional (B2PLYP-D3) instead of the single-hybrid functional (B3LYP) that was previously employed because it generally provides more accurate vibrational frequency predictions for a modest increase in computational cost. 54,55 Augmented double ζ basis sets (AVDZ) were used throughout. Our initial structures (before optimization) correspond to those reported in ref 56, which were calculated at the B3LYP/6-31G(d) level of theory. All harmonic frequencies have been scaled by a factor that was determined by comparing computed and experimental symmetric CD₃ stretching frequencies for the monomer (0.9554).

3. RESULTS AND DISCUSSION

3.1. Methanol Clusters. Figure 1 shows the infrared spectra of methanol- d_3 clusters embedded in superfluid helium nanodroplets at a variety of pickup chamber pressures. At the lowest pressure only the monomer is evident, which is characterized by a somewhat broad envelope centered at 2076.59 cm⁻¹. This envelope contains rotational substructure and has previously been analyzed.³⁸ Upon increasing the pressure, several new peaks grow in, initially at -8 cm^{-1} and $+6 \text{ cm}^{-1}$ relative to the central monomer peak, which is

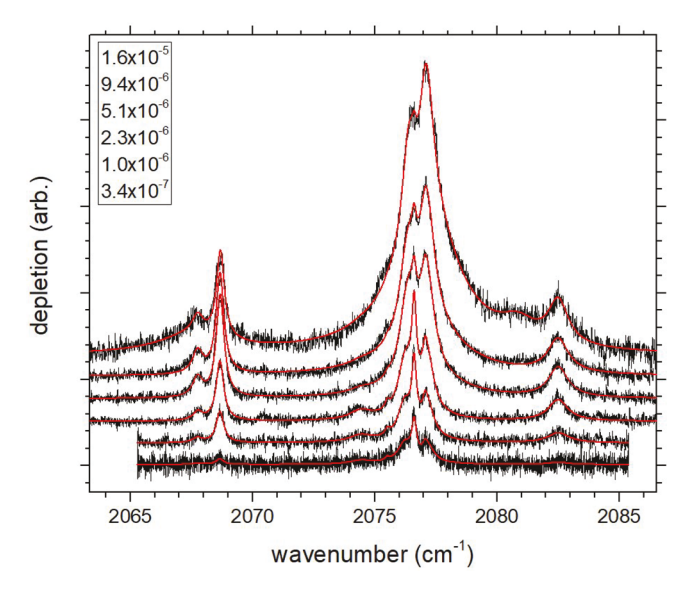


Figure 1. Depletion spectra of methanol- d_3 clusters in the symmetric CD₃ stretching band. The red curves are simulated spectra using the parameters listed in Table 1. The pickup chamber pressure (inset) is in Torr. Note that the (very weak) 2074.4 cm⁻¹ peak corresponds to the methanol- d_4 monomer.³⁸

followed by an increase in the intensity and change in the morphology around where the monomer absorbs. Finally, at the highest pressure, two broad peaks grow in at $-9~{\rm cm}^{-1}$ and $+4~{\rm cm}^{-1}$. All of these features correspond to the symmetric CD₃ stretching vibration, and in the following we analyze each of them and assign them to specific methanol clusters.

In order to uncover all of the significantly intense peaks that are hidden within the spectra, we fit them to the sum of a number of Lorentzian functions. This was previously done for the methanol- d_3 monomer, for which a nonrigid symmetric top energy level equation was used to model the line positions.³ This is the only significant contribution to the lowest pressure spectrum, for which the sum of the Lorentzian functions extends from about 2073 to 2079 $\,\mathrm{cm}^{-1}$ (see bottom trace in Figure 1). For the fits performed here, we fixed the relative line positions and widths of the monomer peaks and only floated the absolute intensity (including a small contribution from methanol- d_4). With increasing pressure, more and more peaks became important to include in the fit; the highest pressure spectrum has the most, and Figure 2 shows a breakdown of a fit to this spectrum. It reveals eight new peaks (on top of the monomer envelope) that can be assigned to methanol clusters.

In helium nanodroplet isolation spectroscopy it is typical to determine the dopant cluster size by recording the depletion signal as a function of partial pressure and fitting the data to Poissonian curves. When peaks are overlapping, however, it becomes problematic, and here we fit the spectra to a sum of Lorentzian peaks (vide supra) and plot of the relative intensity of each peak across the range of partial pressures of methanold₃ investigated (see Figure 3 caption for further details). The evolution in the relative intensity for each peak can then be used to assign cluster sizes, which are listed in Table 1. For the monomer (2076.59 cm⁻¹), which was assigned in ref 38, the relative intensity gradually decreases with increasing pressure. The other peaks are observed to initially increase in relative intensity, and three of them (2067.76, 2068.66, and 2082.50 cm⁻¹) which are correlated with each other grow in the fastest; they are assigned to the dimer. Next, we find that a pair of

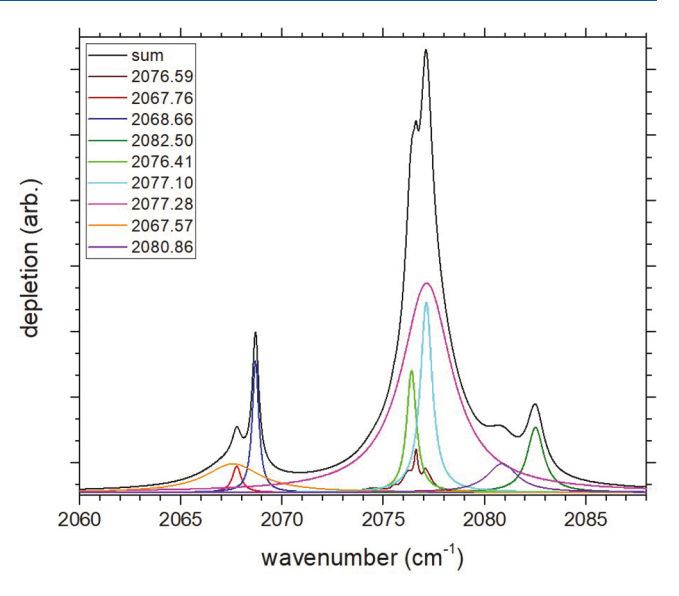


Figure 2. Decomposition of the individual contributions to the fitted spectrum of methanol- d_3 clusters at the highest pickup chamber pressure (see Figure 1). The line positions (inset) are in cm⁻¹.

peaks (2076.41 and 2077.10 cm⁻¹) grow in much slower, which we assign to the trimer. Next, a broad peak (2077.28 cm⁻¹) is observed to gain intensity and gradually increases over the pressure ranges investigated; this is assigned to clusters that contain at least four methanol molecules. Finally, at the highest pressure we see two new broad peaks (2067.57 and 2080.86 cm⁻¹) appear, which we assign to larger clusters yet (probably containing at least six methanol molecules). With cluster sizes assigned to each deconvoluted peak, we turn our attention to gaining some structural insight based on their relative frequency and intensity, as well as from comparison with previous work (experimental and theoretical).

3.1.1. Dimer. The two most intense dimer peaks that become apparent upon tripling the pressure (from 3.4×10^{-7} to 1×10^{-6} Torr) can be assigned to vibrations of the linear dimer; the peak at 2067.76 cm⁻¹ corresponds to vibration of the CD3 stretch within the H-bond donor molecule, and 2082.50 cm⁻¹ corresponds to the same vibration within the Hbond acceptor molecule. This specific assignment was readily made by comparison with a previous investigation of symmetric CH₃ stretch of the *normal* isotopologue of methanol,¹⁹ where the donor and acceptor peaks were observed to be separated by 26 cm⁻¹, which when scaled predicts a splitting of 19 ± 3 cm⁻¹ in the symmetric CD₃ stretch investigated here; Table 1 shows the splitting is marginally less than this at ~14 cm⁻¹. The assignment to donor [acceptor] being at lower [higher] wavenumber was supported by theory. 19,57 Our scaled DFT calculations agree with this but somewhat overpredict the splitting by $\sim 8.5 \text{ cm}^{-1}$, as shown in Figure 4.

The third dimer peak at 2067.76 cm⁻¹ is assigned to the D-bond donor CD₃OD molecule within the linear methanol dimer (CD₃OD-CD₃OH). This assignment was made following the measurement of the depletion spectra of pure methanol- d_4 clusters (also in the symmetric CD₃ stretching band), which are plotted in Figure 5. The lowest frequency peak in these spectra, which initially grows in rapidly and is coincident with the "third dimer peak" in Figure 1, is clearly the D-bond donor CD₃OD molecule within the pure d_4 dimer: Evidently, the isotopologue of methanol accepting the

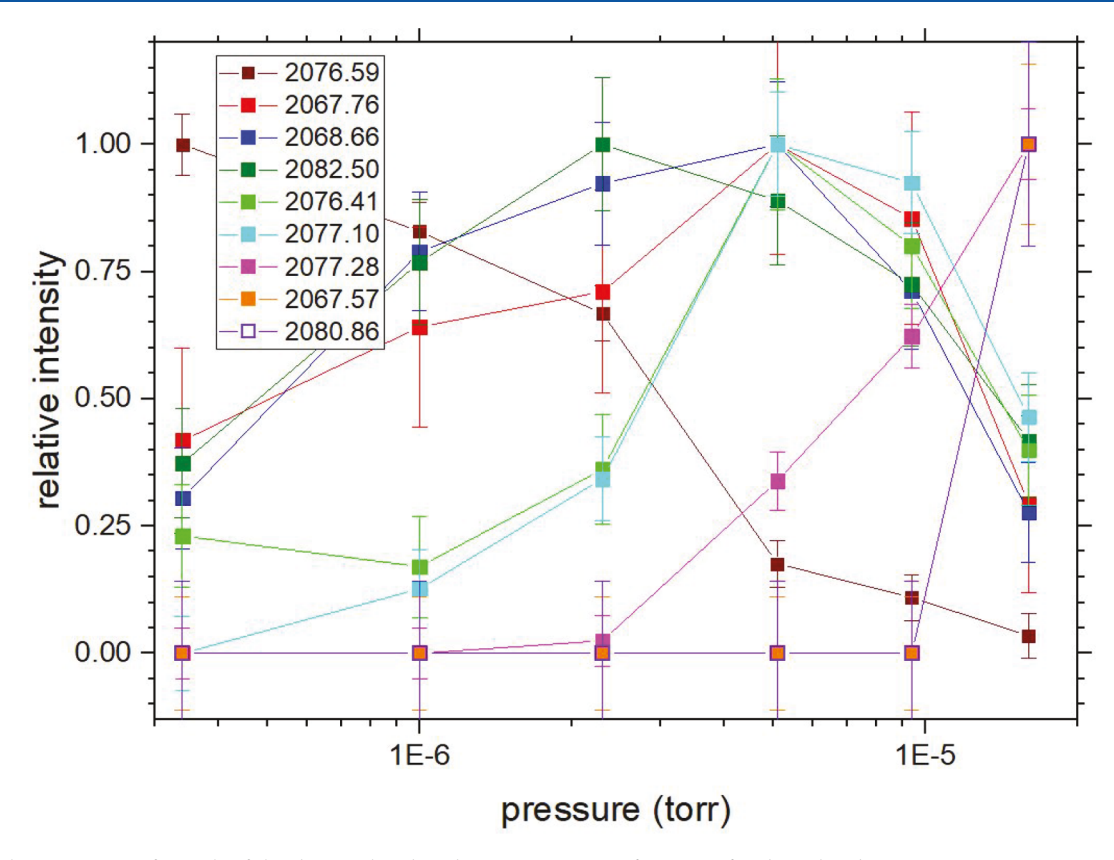


Figure 3. Relative intensity for each of the deconvoluted peaks in Figure 2 as a function of pickup chamber pressure; uncertainties are estimated. The values were determined by (1) normalizing the sum of the peak intensities for each pressure to 1, then (2) multiplying the resulting values for each peak (across all pressures) by a particular factor such that the most intense peak is equal to 1.

Table 1. Line Positions, Widths, and Assignments for Methanol Clusters Embedded in Helium Nanodroplets^a

$\nu (\mathrm{cm}^{-1})$	Γ (cm ⁻¹)	assignment ^a
2067.76(2)	0.24	$d (CD_3OD) - (CD_3OH)$
2068.66(2)	0.19	$d (CD_3OH)_2$
2082.50(5)	0.49	$a (CD_3OH)_2$
2076.41(3)	0.25	$c (CD_3OH)_3$
2077.10(3)	0.35	$c (CD_3OH)_3$
2077.28(17)	1.72	c (CD ₃ OH) ₄₊
2067.57(17)	1.68	$d (CD_3OH)_{5+}$
2080.86(9)	0.90	$a (CD_3OH)_{5+}$

"Uncertainties (in last place) are estimated. Italicized letter indicates type of vibrating methanol in the cluster; d = donor, a = acceptor, and c = cyclic. Only dominant assignment is given.

hydrogen bond has an insignificant effect on the CD_3 stretching vibrational frequency of the donor molecule. The line width of the broad feature near band origin of the monomer that grows in at higher pickup chamber pressures is $\sim 2\times$ greater for CD_3OD than CD_3OH (see inset in Figure 5), suggesting faster vibrational relaxation of larger clusters for d_4 methanol in comparison to d_3 methanol. This is consistent with the previously reported helium nanodroplet isolation spectra of the d_3 and d_4 monomers, for which the rotational substructure was only evident for the d_3 monomer; it was speculated that the substructure was washed out for d_4 methanol on account of the stronger Fermi coupling between the excited symmetric CD_3 stretching vibrational state and a nearby lower energy state. The should be noted that while the choice of using a Gaussian function to fit the "difference"

spectrum" shown in Figure 5 was purely empirical, the good quality of the fit suggests that the observed peak is inhomogeneously broadened. This is consistent with there being underlying substructure, similar to what was deconvoluted in the methanol- d_3 cluster spectra presented above.

3.1.2. Trimer. As can be seen in Figure 2, we observed two trimer peaks (2076.41 and 2077.10 cm⁻¹) near the band origin of the monomer. Previous calculations predict that cyclic cluster peaks should lie in this region, which is around the midpoint of the donor and acceptor methyl stretching vibrations of the linear dimer; 19,58 the two peaks we observed are therefore assigned to the cyclic trimer. There are two isomers of the cyclic trimer that could be responsible for these peaks: they have chair-like and bowl-like structures (see bottom inset in Figure 4). Of them, it is the transiently chiral chair-like isomer that is generally agreed upon to be the most stable (because it minimizes steric repulsion),⁵⁹ This is the one that is typically assigned to trimer peaks in experimental infrared spectra, e.g., in ref 30. In a sensitive cavity ringdown experiment on methanol clusters, additional trimer lines were observed that were tentatively assigned to the bowl-like isomer; 14 however, more recent infrared/Raman experiments indicate that these lines are probably related to low-frequency van der Waals modes of the chair-like cluster. 13

In order to assign the two observed trimer peaks to specific isomers/vibrations, we performed DFT calculations on the two lowest energy trimers (chair-like and bowl-like). Figure 4 compares the calculated spectra of these isomers to the trimer peaks that were deconvoluted from the observed spectra. The two lowest frequency calculated lines for the most stable isomer (chair-like) fall very close to the observed line positions

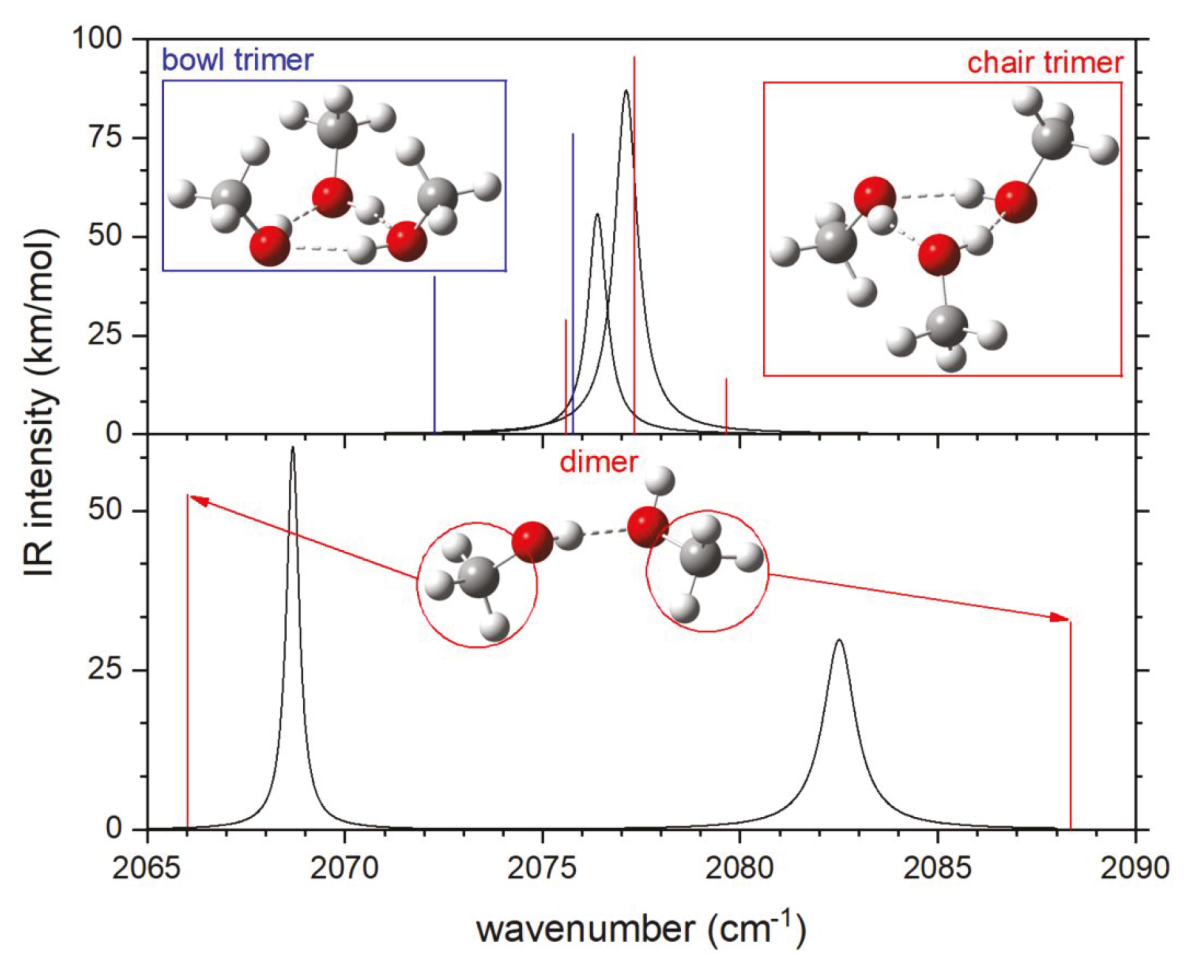


Figure 4. Bottom: Deconvoluted dimer peaks in comparison with the calculated spectrum. Top: Deconvoluted trimer peaks in comparison with the calculated spectra of the two lowest energy isomers.

(<1 cm⁻¹ away) and have an intensity ratio (1:3) that is roughly consistent with the observations (1:2). We speculate that the slightly higher relative intensity of the observed lower frequency line than predicted is an artifact that results from the d_4 impurity in the d_3 sample. The predictions for the bowllike isomer (see Figure 4) are significantly farther away from the observations, and so we assign the two observed trimer peaks to the chair-like isomer. Similar to the case of the dimer (*vide supra*), the predicted splitting of the trimer peaks is greater than what was observed. We note that there is a predicted high frequency line for this isomer that we do not observe; however it is expected to be relatively weak (which we speculate is the reason for its nonidentification).

3.1.3. Larger Clusters. Upon turning our attention to larger clusters (>3 molecules), we deconvoluted one relatively broad peak from the experimental spectra that overlaps with the monomer and trimer peaks (see Figure 2). This broad peak grows in intensity more slowly than the trimer peaks (see Figure 3), which is consistent with it corresponding to clusters that consist of at least four methanol molecules. It seems reasonable that these clusters are cyclic, since the shift is close to 0 cm⁻¹ from the cyclic trimer peaks. This is in agreement with our DFT calculations, which predict a shift of less than 2 cm⁻¹ relative to the monomer for the most intense frequency peak for each of the cyclic clusters (3–6 molecules); see the Supporting Information. Figure 6 shows the predicted spectra of larger cyclic methanol clusters (4–6 molecules), which show

good general agreement with the broad experimental larger cluster peak that we observed. There are two remaining peaks that grow in at even higher pickup chamber pressures, and based on their intensity dependence on the methanol partial pressure (Figure 3), they must correspond to clusters that consist of at least five methanol molecules. They are both located within 2 cm⁻¹ of the donor and acceptor peaks of the dimer (at -9 and +4 cm⁻¹ relative to the monomer), suggesting their bonding character is similar. We assign them to the donor (to the red) and acceptor (to the blue) molecules in branched clusters that probably have a cyclic core. Unfortunately we are unable to determine the exact number of methanol molecules in these branched clusters but suspect they contain at least six molecules because only the cyclic pentamer was detected in helium nanodroplets in ref 36. In order to test this hypothesis, we calculated the vibrational frequencies of a low energy branched hexamer, which does indeed show a low and high frequency peak with reasonably strong intensities that fall within 2 cm⁻¹ of the observed low and high frequency peaks (see Figure 6).

To close this subsection, we present spectra in the CD_3 stretching band where we have intentionally co-doped the nanodroplets with comparable amounts of CD_3OH and CD_3OD (see Figure 7). The dimer peaks to the red of the monomer are the most sensitive indicator of what isotopologue is acting as a donor. At similar partial pressures, the intensity of the H-bond donor and D-bond donor stretching bands is

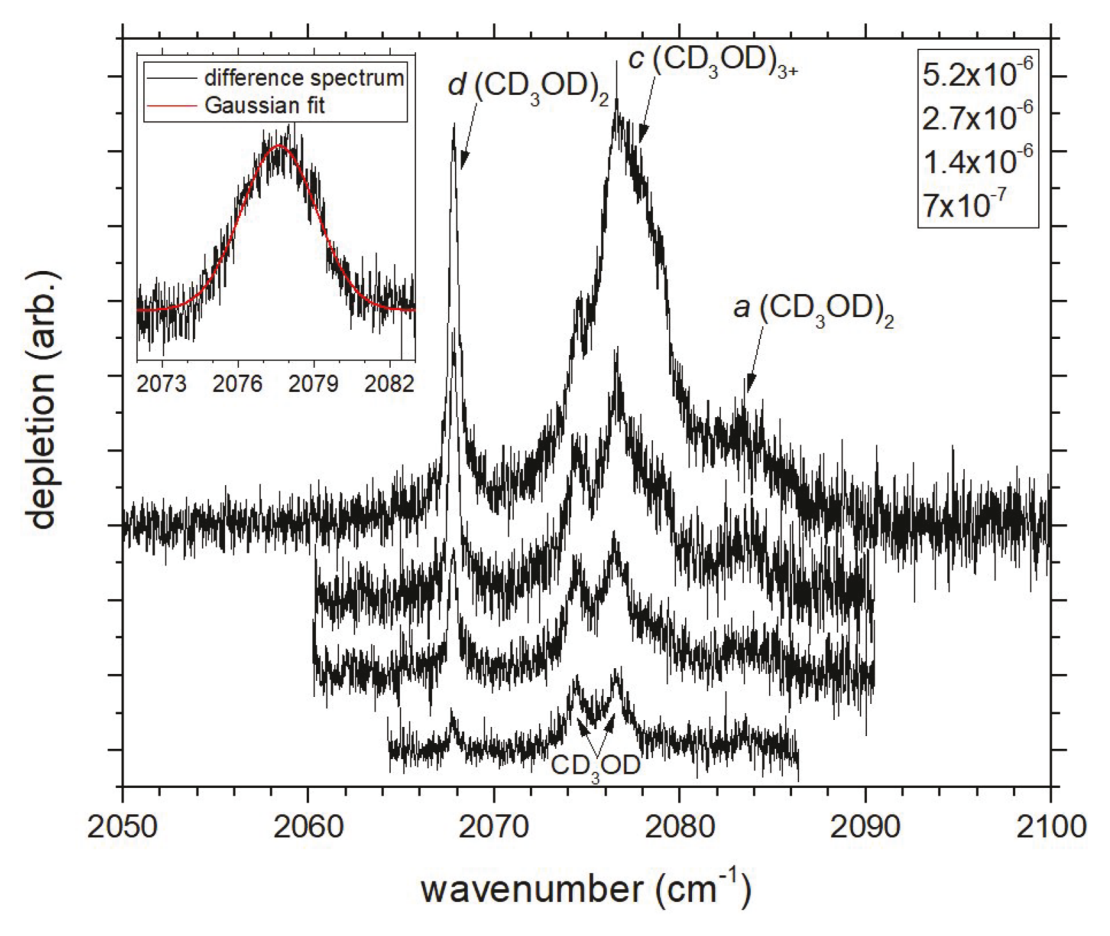


Figure 5. Same as Figure 1 but for methanol- d_4 clusters. The inset shows a difference spectrum between the highest pressure and the lowest pressure (×2) along with a Gaussian fit ($\nu = 2077.6 \text{ cm}^{-1}$; $\Gamma = 3.5 \text{ cm}^{-1}$).

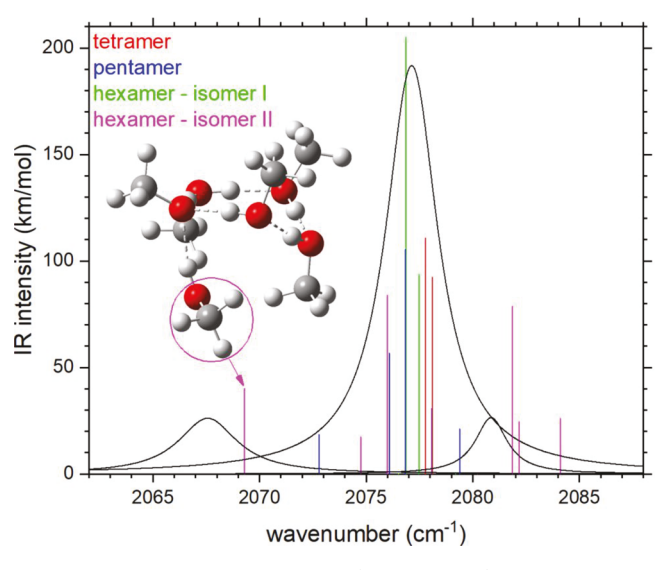


Figure 6. Deconvoluted $N \ge 4$ peak (strongest one) and $N \ge 5$ peaks in comparison with the calculated spectra for the lowest energy tetramer, pentamer, and hexamer isomers in addition to a branched hexamer [chaise pentamer + 1; it is very similar to the lowest energy branched hexamer (isomer 7) found in ref 61].

similar. When the partial pressure of CD₃OH is doubled, the intensity of the H-bond donor stretching bands approximately doubles, indicating no significant preference for formation of

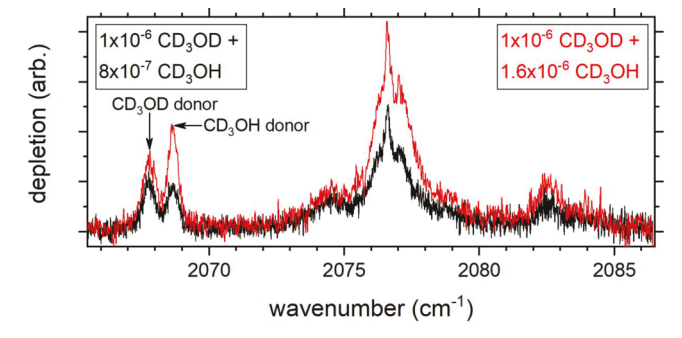


Figure 7. Depletion spectra of mixed methanol- d_3 and methanol- d_4 clusters in the symmetric CD₃ stretching band. The positions of the donor bands of the isotopolologues of the methanol dimer are arrowed.

 $(CD_3OD)-(CD_3OH)$ over $(CD_3OH)-(CD_3OD)$ [as might be expected based on zero-point effects].

3.2. Methanol–Water Clusters. In Figure 8 we show the spectra of CD_3OH at a relatively low pickup pressure in comparison to spectra where we have slowly increased the partial pressure of H_2O in the pickup chamber. At the lowest pressure the monomer and a lesser amount of dimer are evident. With an increasing partial pressure of water, the intensity of the monomer and "bound" dimer peaks decreases, the latter of which occurs at a seemingly faster rate. At a water partial pressure of 2.3×10^{-6} Torr, the bound dimer peak has disappeared and nothing new has grown in to the red of the

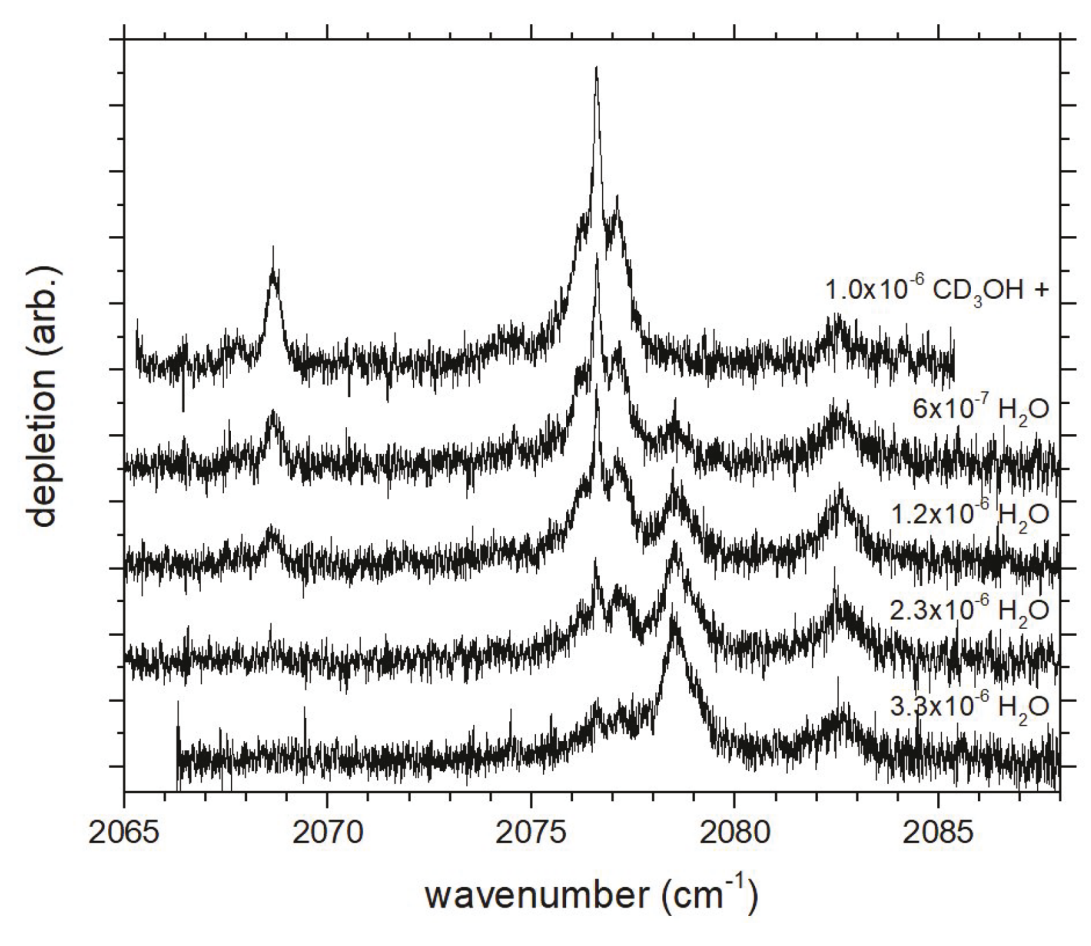


Figure 8. Depletion spectra of methanol-d₃-water clusters in the symmetric CD₃ stretching band.

monomer. This suggests that methanol is not acting as a H-bond donor with sufficient water present. On the other hand, the intensity of the peak at $\sim\!2082.5~{\rm cm}^{-1}$ is slightly greater at this higher pressure. Since the H-bond donor methanol dimer peak disappeared in going to 2.3×10^{-6} Torr of water, the peak at $2082.5~{\rm cm}^{-1}$ must now correspond to the H-bond acceptor methanol in the water—methanol complex. The structure of the water—methanol complex is thus consistent with methanol acting as a H-bond acceptor in the methanol—water dimer, which is not surprising since it has been calculated to lie lower in energy than the dimer with water acting as an acceptor, 62 and it is the only structural isomer of the dimer that has been observed both in the gas phase 63 and in helium nanodroplets. 64

In addition to the H-bond acceptor dimer peak that initially grows in at elevated water partial pressures, a new feature gains intensity at 2078.5 cm $^{-1}$, and unlike the dimer peak, it continues to increase in intensity as a function of water partial pressure (beyond 1.2×10^{-6} Torr). On account of it being only ~ 2 cm $^{-1}$ to the blue of the monomer band origin, we assign it to cyclic clusters with at least 2 water molecules. If we begin with a 5× higher pressure of CD₃OH (see Figure 9), a similar progression is observed upon increasing the water partial pressure, with the peak at 2078.5 cm $^{-1}$ dominating the spectrum at the highest pressures used. Since we initially begun with larger methanol clusters (on average), the dominant peak at higher pressures must correspond to a wide variety of cyclic methanol—water complexes. This finding is consistent with previous helium nanodroplet isolation spectroscopy experi-

ments which focused in the OH stretching region, as discussed in the following. 36

3.3. Comparison with Previous Spectroscopy in Helium Nanodroplets. The high resolution IR spectra of helium solvated methanol monomers ^{38,65} and clusters ^{35,36} have previously been reported, in addition to that for mixed methanol—water clusters. ^{36,64} Different spectroscopic regions were investigated for each type: methanol monomers in the CO, CH, and OH stretching regions, methanol clusters in the CO and OH stretching regions, and mixed clusters in the OH stretching region.

We begin with a comparison of the spectra of helium solvated methanol clusters. As mentioned above, the OH stretching region is most sensitive to the presence of H-bonds between molecules, as evidenced by the largest frequency shifts upon their formation. Sulaiman et al. investigated clusters ranging in size from the dimer to the pentamer and found that there is indeed a large red shift for most bands and that its magnitude increases with cluster size.³⁶ This, along with the closeness in proximity to band positions observed for bare clusters from both cavity ring down 14 and FTIR 11 spectroscopies, allowed for assignments to be readily made to cyclic structures (from trimer to pentamer). Our analysis of the qc laser spectra reported here are consistent with these assignments, and additionally reveal peaks that we assigned to Hbond donor and acceptor molecules in branched clusters (that consist of at least five methanol molecules). Branched clusters have been assigned to peaks in the CO stretching spectra of smaller methanol clusters in helium nanodroplets;³⁵ however,

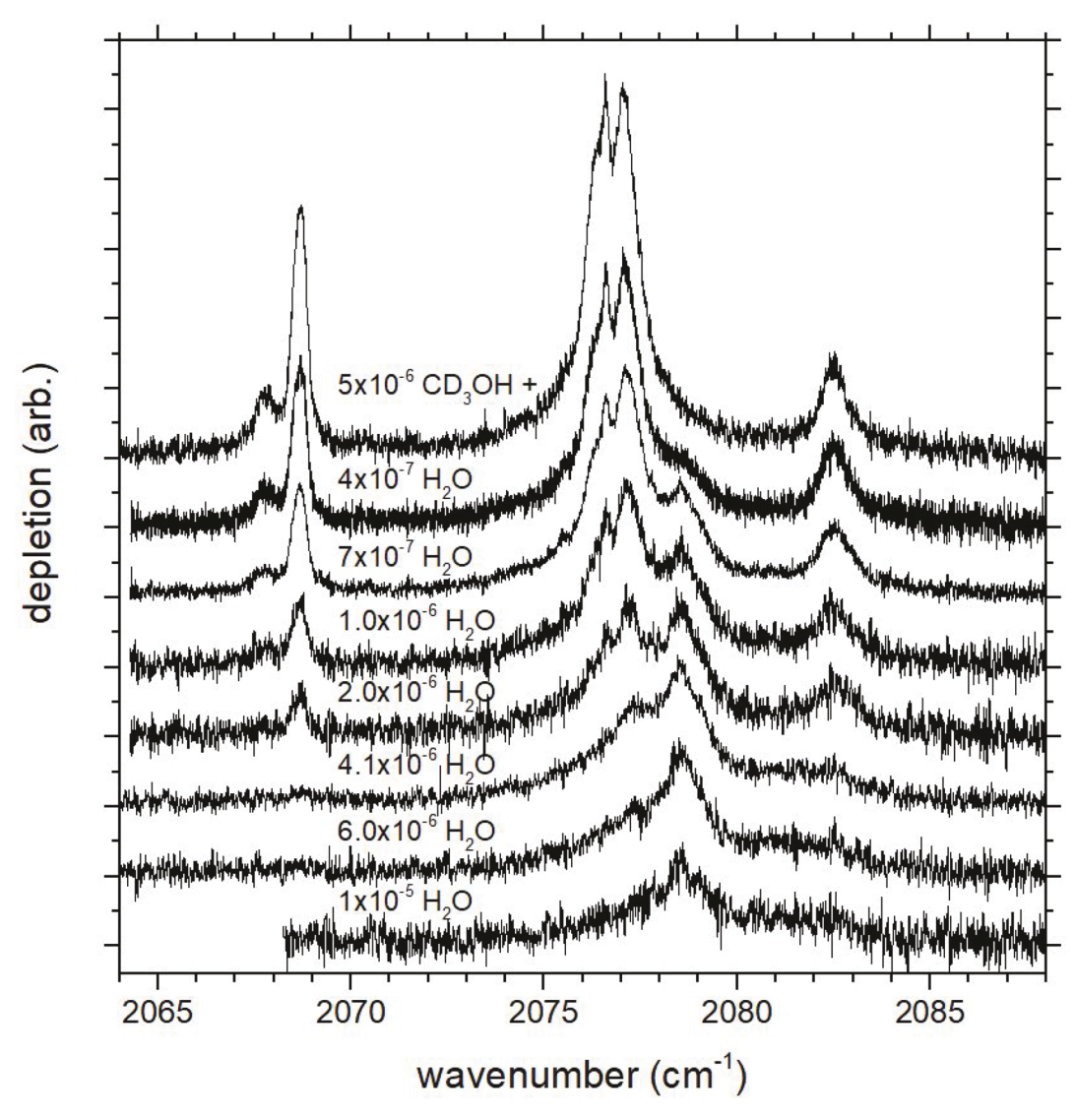


Figure 9. Similar to Figure 8 but with a 5× higher partial pressure of methanol- d_3 .

those assignments are not consistent with the more recent investigation in the OH stretching region. 36

Next, we compare the helium nanodroplet isolation spectra of mixed clusters reported here with the previous investigation that focused on the OH stretching region of methanol. In the previous investigation of mixed clusters in helium nanodroplets the relative partial pressure of water in the pickup chamber was kept low so that the probed clusters contained no more than one water molecule. This differs from the experiments described here, which generally favor formation of clusters containing more water molecules than methanol (at least at higher pickup chamber pressures). Despite this, in both investigations only cyclic mixed clusters for the trimer (and above) have been observed (no evidence for branched mixed clusters has been found to date). Additionally, as mentioned above, observation of methanol acting as a H-bond acceptor in the methanol-water dimer is in agreement with the helium nanodroplet isolation spectrum of it in the OH stretching region.64

4. SUMMARY AND OUTLOOK

Here we performed laser spectroscopy in the symmetric CD₃ stretching band of methanol clusters and mixed methanolwater clusters in order to see if it can be used to explore their structures. We found that although the vibrational frequency shift is relatively small between different cluster sizes (and isomers), this band is indeed a somewhat sensitive probe. For the methanol dimer, we observe a strong [weak] band to the red [blue] of the monomer that corresponds to the donor [acceptor] molecule. For the methanol trimer, tetramer, and pentamer, peaks are evident near that of the monomer, which are shown (with the help of vibrational frequency calculations) to correspond to cyclic structures, in agreement with a recent investigation.³⁶ For larger clusters we observed two broad peaks, one near each of the donor and acceptor bands of the methanol dimer. We assign these to donor and acceptor vibrations in branched clusters with a cyclic core. Regarding mixed methanol-water clusters, we find that the dimer adopts its minimum energy structure, with the water acting as the hydrogen-bond donor. This is evidenced by an increase in intensity of the acceptor vibration of methanol relative to the donor vibration with addition of water to CD₃OH doped

droplets. For larger mixed clusters, we observe a broad peak near the band origin of the methanol monomer, suggesting that they are largely cyclic. Future experiments focusing on a spectral region with less homogeneous broadening could be useful, perhaps in the CO stretching region where (at least) the monomer lines are much sharper, of and rotationally resolved spectra could potentially be observed with a narrow line width laser.

ASSOCIATED CONTENT

Supporting Information

The Supporting Information is available free of charge at https://pubs.acs.org/doi/10.1021/acs.jpca.2c08327.

Cartesian coordinates and vibrational frequencies/ intensities of optimized methanol clusters from the B2PLYP-D3/AVDZ calculations (Table S1) (PDF)

AUTHOR INFORMATION

Corresponding Author

Paul L. Raston — Department of Chemistry, University of Adelaide, Adelaide, SA 5005, Australia; Department of Chemistry and Biochemistry, James Madison University, Harrisonburg, Virginia 22807, United States; occid.org/0000-0003-3717-4154; Email: rastonpl@jmu.edu

Author

Maameyaa Asiamah — Department of Chemistry and Biochemistry, James Madison University, Harrisonburg, Virginia 22807, United States

Complete contact information is available at: https://pubs.acs.org/10.1021/acs.jpca.2c08327

Notes

The authors declare no competing financial interest.

ACKNOWLEDGMENTS

We acknowledge support from the National Science Foundation (Grants NSF-REU CHE-1757874 and NSF-CAREER CHE-2141774). This research utilized supercomputing resources provided by the Phoenix HPC service at the University of Adelaide.

REFERENCES

- (1) Errington, J. R.; Debenedetti, P. G. Relationship between structural order and the anomalies of liquid water. *Nature* **2001**, 409 (6818), 318–321.
- (2) Panman, M. R.; Shaw, D. J.; Ensing, B.; Woutersen, S. Local Orientational Order in Liquids Revealed by Resonant Vibrational Energy Transfer. *Phys. Rev. Lett.* **2014**, *113* (20), 207801.
- (3) Pierce, W. C.; MacMillan, D. P. X-ray Studies on Liquids: the Inner Peak for Alcohols and Acids. *J. Am. Chem. Soc.* **1938**, *60* (4), 779–783.
- (4) Pauling, L. The Nature of the Chemical Bond; Cornell University Press: Ithaca, NY, 1960.
- (5) Jorgensen, W. L. Quantum and statistical mechanical studies of liquids. 7. Structure and properties of liquid methanol. *J. Am. Chem. Soc.* **1980**, *102* (2), 543–549.
- (6) Ludwig, R. The Structure of Liquid Methanol. *ChemPhysChem* **2005**, *6* (7), 1369–1375.
- (7) Guo, J. H.; Luo, Y.; Augustsson, A.; Kashtanov, S.; Rubensson, J. E.; Shuh, D. K.; Agren, H.; Nordgren, J. Molecular structure of alcohol-water mixtures. *Phys. Rev. Lett.* **2003**, *91* (15), 157401.

- (8) Lin, K.; Zhou, X.; Luo, Y.; Liu, S. The Microscopic Structure of Liquid Methanol from Raman Spectroscopy. *J. Phys. Chem. B* **2010**, 114 (10), 3567–3573.
- (9) Lovas, F. J.; Belov, S. P.; Tretyakov, M. Y.; Stahl, W.; Suenram, R. D. The a-Type K = 0 Microwave Spectrum of the Methanol Dimer. *J. Mol. Spectrosc.* **1995**, *170* (2), 478–492.
- (10) Lovas, F. J.; Hartwig, H. The Microwave Spectrum of the Methanol Dimer for K= 0 and 1 States. *J. Mol. Spectrosc.* **1997**, *185* (1), 98–109.
- (11) Häber, T.; Schmitt, U.; Suhm, M. A. FTIR-spectroscopy of molecular clusters in pulsed supersonic slit-jet expansions. *Phys. Chem. Chem. Phys.* **1999**, *1* (24), 5573–5582.
- (12) Wugt Larsen, R.; Suhm, M. A. Cooperative organic hydrogen bonds: The librational modes of cyclic methanol clusters. *J. Chem. Phys.* **2006**, *125* (15), 154314.
- (13) Larsen, R. W.; Zielke, P.; Suhm, M. A. Hydrogen-bonded OH stretching modes of methanol clusters: A combined IR and Raman isotopomer study. *J. Chem. Phys.* **2007**, *126* (19), 194307.
- (14) Provencal, R. A.; Paul, J. B.; Roth, K.; Chapo, C.; Casaes, R. N.; Saykally, R. J.; Tschumper, G. S.; Schaefer, H. F., III. Infrared cavity ringdown spectroscopy of methanol clusters: Single donor hydrogen bonding. *J. Chem. Phys.* **1999**, *110* (9), 4258–4267.
- (15) Provencal, R. A.; Casaes, R. N.; Roth, K.; Paul, J. B.; Chapo, C. N.; Saykally, R. J.; Tschumper, G. S.; Schaefer, H. F. Hydrogen Bonding in Alcohol Clusters: A Comparative Study by Infrared Cavity Ringdown Laser Absorption Spectroscopy. *J. Phys. Chem. A* **2000**, *104* (7), 1423–1429.
- (16) Buck, U.; Huisken, F. Infrared Spectroscopy of Size-Selected Water and Methanol Clusters. *Chem. Rev.* **2000**, *100* (11), 3863–3890.
- (17) Buck, U.; Huisken, F. Infrared Spectroscopy of Size-Selected Water and Methanol Clusters. *Chem. Rev.* **2001**, *101* (1), 205–206.
- (18) Fu, H. B.; Hu, Y. J.; Bernstein, E. R. IR+vacuum ultraviolet (118 nm) nonresonant ionization spectroscopy of methanol monomers and clusters: Neutral cluster distribution and size-specific detection of the OH stretch vibrations. *J. Chem. Phys.* **2006**, *124* (2), No. 024302.
- (19) Han, H.-L.; Camacho, C.; Witek, H. A.; Lee, Y.-P. Infrared absorption of methanol clusters (CH₃OH)n with n = 2–6 recorded with a time-of-flight mass spectrometer using infrared depletion and vacuum-ultraviolet ionization. *J. Chem. Phys.* **2011**, *134* (14), 144309.
- (20) Zwier, T. S. The spectroscopy of solvation in hydrogen-bonded aromatic clusters. *Annu. Rev. Phys. Chem.* **1996**, 47 (1), 205–241.
- (21) Ebata, T.; Fujii, A.; Mikami, N. Vibrational spectroscopy of small-sized hydrogen-bonded clusters and their ions. *Int. Rev. Phys. Chem.* **1998**, 17 (3), 331–361.
- (22) Buck, U. Infrared Spectroscopy of Size-Selected Molecular Clusters. In *Advances in Atomic, Molecular, and Optical Physics*; Bederson, B., Walther, H., Eds.; Academic Press, 1995; Vol. 35, pp 121–161.
- (23) Buck, U.; Gu, X. J.; Lauenstein, C.; Rudolph, A. Infrared photodissociation of size-selected methanol clusters. *J. Chem. Phys.* **1990**, 92 (10), 6017–6029.
- (24) Huisken, F.; Stemmler, M. Infrared photodissociation of small methanol clusters. *Chem. Phys. Lett.* **1988**, *144* (4), 391–395.
- (25) Huisken, F.; Stemmler, M. Infrared molecular beam depletion spectroscopy of size-selected methanol clusters. *Zeitschrift für Physik D Atoms, Molecules and Clusters* **1992**, 24 (3), 277–287.
- (26) Buck, U.; Ettischer, I. Vibrational predissociation spectra of size selected methanol clusters: New experimental results. *J. Chem. Phys.* **1998**, *108* (1), 33–38.
- (27) Buck, U.; Hobein, M. IR double resonance experiments with size selected clusters for identification of isomers. *Zeitschrift für Physik D Atoms, Molecules and Clusters* **1993**, 28 (4), 331–337.
- (28) Buck, U.; Gu, X.; Lauenstein, C.; Rudolph, A. Infrared photodissociation spectra of size-selected (CH3OH)n clusters from n = 2 to n = 8. *J. Phys. Chem.* **1988**, 92 (20), 5561–5562.

- (29) Huisken, F.; Kulcke, A.; Laush, C.; Lisy, J. M. Dissociation of small methanol clusters after excitation of the O–H stretch vibration at 2.7 μ . *J. Chem. Phys.* **1991**, *95* (6), 3924–3929.
- (30) Huisken, F.; Kaloudis, M.; Koch, M.; Werhahn, O. Experimental study of the O-H ring vibrations of the methanol trimer. *J. Chem. Phys.* **1996**, *105* (19), 8965–8968.
- (31) Odutola, J. A.; Viswanathan, R.; Dyke, T. R. Molecular beam electric deflection behavior and polarity of hydrogen-bonded complexes of ROH, RSH, and RNH. *J. Am. Chem. Soc.* **1979**, *101* (17), 4787–4792.
- (32) Hartmann, M.; Miller, R. E.; Toennies, J. P.; Vilesov, A. Rotationally Resolved Spectroscopy of Sf6 in Liquid-Helium Clusters a Molecular Probe of Cluster Temperature. *Phys. Rev. Lett.* **1995**, 75 (8), 1566–1569.
- (33) Nauta, K.; Miller, R. E. Nonequilibrium self-assembly of long chains of polar molecules in superfluid helium. *Science* **1999**, 283 (5409), 1895–1897.
- (34) Nauta, K.; Miller, R. E. Formation of cyclic water hexamer in liquid helium: The smallest piece of ice. *Science* **2000**, 287 (5451), 293–295.
- (35) Behrens, M.; Frochtenicht, R.; Hartmann, M.; Siebers, J. G.; Buck, U.; Hagemeister, F. C. Vibrational spectroscopy of methanol and acetonitrile clusters in cold helium droplets. *J. Chem. Phys.* **1999**, 111 (6), 2436–2443.
- (36) Sulaiman, M. I.; Yang, S.; Ellis, A. M. Infrared Spectroscopy of Methanol and Methanol/Water Clusters in Helium Nanodroplets: The OH Stretching Region. *J. Phys. Chem. A* **2017**, *121* (4), 771–776.
- (37) Faulkner, T.; Miller, I.; Raston, P. L. Quantum Cascade Laser Spectroscopy of OCS Isotopologues in ⁴He Nanodroplets: A Test of Adiabatic Following for a Heavy Rotor. *J. Chem. Phys.* **2018**, *148* (4), No. 044308.
- (38) Miller, I.; Faulkner, T.; Raston, P. L. Laser Spectroscopy of Methanol Isotopologues in ⁴He Nanodroplets: Probing the Inertial Response around a Moderately Light Rotor. *J. Phys. Chem. A* **2019**, 123 (8), 1630–1636.
- (39) Miller, I.; Faulkner, T.; Saunier, J.; Raston, P. L. Observation of the elusive "oxygen-in" OCS dimer. *J. Chem. Phys.* **2020**, *152* (22), 221102.
- (40) Raston, P. L. Helium nanodroplet isolation spectroscopy in an undergraduate teaching laboratory. *J. Mol. Spectrosc.* **2022**, 388, 111676
- (41) Knuth, E.; Schilling, B.; Toennies, J. P. Proceedings of the 19th International Symposium on Rarefied Gas Dynamics; Oxford University Press: London, 1995.
- (42) Raston, P. L. HeNDS: A program for calculating average Helium NanoDroplet Sizes. *SoftwareX* **2021**, *14*, 100703.
- (43) Toennies, J. P.; Vilesov, A. F. Spectroscopy of atoms and molecules in liquid helium. *Annu. Rev. Phys. Chem.* **1998**, 49, 1–41.
- (44) Callegari, C.; Lehmann, K. K.; Schmied, R.; Scoles, G. Helium nanodroplet isolation rovibrational spectroscopy: Methods and recent results. *J. Chem. Phys.* **2001**, *115* (22), 10090–10110.
- (45) Toennies, J. P.; Vilesov, A. F. Superfluid Helium Droplets: A Uniquely Cold Nanomatrix for Molecules and Molecular Complexes. *Angew. Chem., Int. Ed.* **2004**, 43 (20), 2622–2648.
- (46) Choi, M. Y.; Douberly, G. E.; Falconer, T. M.; Lewis, W. K.; Lindsay, C. M.; Merritt, J. M.; Stiles, P. L.; Miller, R. E. Infrared spectroscopy of helium nanodroplets: novel methods for physics and chemistry. *Int. Rev. Phys. Chem.* **2006**, 25 (1–2), 15–75.
- (47) Stienkemeier, F.; Lehmann, K. K. Spectroscopy and dynamics in helium nanodroplets. J. Phys. B 2006, 39 (8), R127-R166.
- (48) Kupper, J.; Merritt, J. M. Spectroscopy of free radicals and radical containing entrance-channel complexes in superfluid helium nanodroplets. *Int. Rev. Phys. Chem.* **2007**, *26* (2), 249–287.
- (49) Szalewicz, K. Interplay Between Theory and Experiment in Investigations of Molecules Embedded in Superfluid Helium Nanodroplets. *Int. Rev. Phys. Chem.* **2008**, *27* (2), 273–316.
- (50) Yang, S.; Ellis, A. M. Helium droplets: a chemistry perspective. *Chem. Soc. Rev.* **2013**, 42 (2), 472–484.

- (51) Verma, D.; Tanyag, R. M. P.; O'Connell, S. M. O.; Vilesov, A. F. Infrared spectroscopy in superfluid helium droplets. *Adv. Phys.: X* **2019**, *4* (1), 1553569.
- (52) Raston, P. L. Laser spectroscopy of helium solvated molecules: probing the inertial response. *Phys. Chem. Chem. Phys.* **2021**, 23 (45), 25467–25479.
- (53) Frisch, M. J.; Trucks, G. W.; Schlegel, H. B.; Scuseria, G. E.; Robb, M. A.; Cheeseman, J. R.; Scalmani, G.; Barone, V.; Mennucci, B.; Petersson, G. A.; et al. *Gaussian 09*; Gaussian, Inc.: Wallingford, CT, U.S., 2009.
- (54) Howard, J. C.; Enyard, J. D.; Tschumper, G. S. Assessing the accuracy of some popular DFT methods for computing harmonic vibrational frequencies of water clusters. *J. Chem. Phys.* **2015**, *143* (21), 214103.
- (55) Hull, K.; Soliday, R. M.; Raston, P. L. FIR spectroscopy and DFT calculations involving 2-chloroethanol: Analysis of the ν_{19} + $\nu_{21}\nu_{21}$ torsional hot band, and the solvated substitution reaction between ethylene glycol and hydrogen chloride. *J. Mol. Struct.* **2020**, 1217, 128369.
- (56) Boyd, S. L.; Boyd, R. J. A Density Functional Study of Methanol Clusters. *J. Chem. Theory Comput.* **2007**, *3* (1), 54–61.
- (57) Nishimura, Y.; Lee, Y.-P.; Irle, S.; Witek, H. A. Critical interpretation of CH– and OH– stretching regions for infrared spectra of methanol clusters (CH₃OH)n (n = 2–5) using self-consistent-charge density functional tight-binding molecular dynamics simulations. *J. Chem. Phys.* **2014**, *141* (9), No. 094303.
- (58) Mó, Ó.; Yáñez, M.; Elguero, J. Study of the methanol trimer potential energy surface. J. Chem. Phys. 1997, 107 (9), 3592–3601.
- (59) George, W. O.; Jones, B. F.; Lewis, Rh. Water and its homologues: a comparison of hydrogen bonding phenomena. *Philos. Trans. R. Soc., A* **2001**, 359 (1785), 1611–1629.
- (60) This seems reasonable given that the frequency difference between the two trimer peaks is \sim 0.7 cm⁻¹, which is similar to the difference between the low frequency dimer lines (0.9 cm⁻¹), labeled "d (CD₃OD)–(CD₃OH)" and "d (CD₃OH)₂" in Table 1. Taking into consideration the amount of d_4 impurity in the sample as discussed in the main text, this could account for roughly half of the intensity of the lowest frequency trimer peak.
- (61) Boda, M.; Patwari, G. N. Internal electric fields in methanol [MeOH]₂₋₆ clusters. *Phys. Chem. Chem. Phys.* **2020**, 22 (19), 10917–10923.
- (62) Lee, Y.-F.; Kelterer, A.-M.; Matisz, G.; Kunsági-Máté, S.; Chung, C.-Y.; Lee, Y.-P. Infrared absorption of methanol-water clusters (CH3OH)n(H2O), n = 1–4, recorded with the VUV-ionization/IR-depletion technique. *J. Chem. Phys.* **2017**, *146* (14), 144308.
- (63) Stockman, P. A.; Blake, G. A.; Lovas, F. J.; Suenram, R. D. Microwave rotation-tunneling spectroscopy of the water—methanol dimer: Direct structural proof for the strongest bound conformation. *J. Chem. Phys.* **1997**, *107* (10), 3782–3790.
- (64) Hernandez, F. J.; Brice, J. T.; Leavitt, C. M.; Pino, G. A.; Douberly, G. E. Infrared Spectroscopy of OH-CH₃OH: Hydrogen-Bonded Intermediate Along the Hydrogen Abstraction Reaction Path. *J. Phys. Chem. A* **2015**, *119* (29), 8125–8132.
- (65) Raston, P. L.; Douberly, G. E.; Jäger, W. Single and Double Resonance Spectroscopy of Methanol Embedded in Superfluid Helium Nanodroplets. *J. Chem. Phys.* **2014**, *141* (4), No. 044301.